City and Environment Interactions 24 (2024) 100170

Contents lists available at ScienceDirect

City and Environment Interactions

journal homepage: www.sciencedirect.com/journal/city-and-environment-interactions

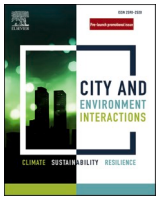

Research Articles

DeNOxing the air in urban spaces by building and construction photocatalytic coverings

J. Fernández-Pampillón [a,b,*], M. Palacios [a], L. Núñez [a], M. Pujadas [a]

[a] Department of Environment, Research Centre for Energy, Environment and Technology (CIEMAT), 28040 Madrid, Spain
[b] Doctoral School, Department of Inorganic Chemistry and Technical Chemistry, Faculty of Sciences, National Distance Education University (UNED), 28040 Madrid, Spain

ARTICLE INFO

Keywords:
DeNOxing
Urban NO_x
Photocatalytic covering

ABSTRACT

A variety of air depolluting TiO_2-based marketed products were applied on bituminous mixtures, sidewalk pavements and facades, giving NO_x oxidation ratios under ISO 22197–1:2007 in the 35–9%, 56–2% and 28–2% ranges, respectively. Correspondingly, $DeNO_x$ toxicity indexes varied from −0.8 to 5.6, 0 to 14 and −4 to 1 μmol.

The three most efficient photocatalytic products were selected: two TiO_2-water dispersions, for road and sidewalk, and a TiO_2-covering, for facade. NO_x purifying ability of these materials were evaluated when key physical parameters were modified. The observed NO_x conversion is positively correlated with UV-A irradiance up to 10 W/m^2, reaching a plateau, and negatively correlated with relative humidity, with a more pronounced decrease above 35%. Inversely, no dependence with inlet NO_x concentration is observed in the range of 0.14–1 ppm_v.

Further, two first-order kinetic approximations were followed to calculate NO surface deposition rates, giving 2 to 8 10^{-3} m/s on the selected photocatalytic urban surfaces. Subsequently, the potential NO_x sink effect induced in a photocatalytic urban canyon and a NO_x-purifier was modelled taking NO_x surface deposition rates from 10^{-3} to 10^{-1} m/s. Purifying devices could be utilised as a preferred option to help alleviate local atmospheric NO_x in high-polluted areas.

Introduction

In Europe, air pollution is a major concern due to its impact on health and environment. On the one hand, the deterioration of the environment due to human activity brings about and aggravates cardiovascular and respiratory diseases. More specifically, the most common causes of premature death associated with air pollution are heart and lung diseases. As an additional consequence, the economy is affected by generated lost working days and high health care costs. On the other hand, ecosystems are also impacted by excessive levels of certain air pollutants as ozone, nitrogen oxides, organic compounds and particulate matter [1].

The EU proposes following a policy to achieve the goal of zero air pollution in 2050 based on bringing ambient air quality standards closer to WHO guidelines, reducing polluting emissions into the atmosphere and controlling the main emission sources [2,3]. Despite the significant reduction in pollutants as a result of the measures adopted, serious air pollution problems still persist [1].

Through Air Quality Directive, the EU regulates the atmospheric levels of particles, tropospheric ozone and nitrogen oxides (NO_x = $NO+NO_2$), among other key pollutants [4]. In particular, certain environmental problems such as the production of ozone in the troposphere, global warming or acid rain, have NO_x as a relevant precursor agent, which can also cause a deterioration in human's health, mainly the respiratory system [5].

In 2020, NO_x emissions from the EU-27 fell by 48% since 2005, with road transport being the main source, responsible for 37% of emissions. Despite efforts, the annual NO_2 limit value (average of 40 $\mu g/m^3$) is frequently surpassed at critical traffic points in urban areas due to accumulated emissions from road traffic, a situation recorded in 2% of the air quality monitoring stations, of which 69% are traffic stations [1].

Air quality plans contemplate various strategies aimed at reducing air pollution in cities. The heterogeneous photocatalysis process is the basis of construction materials that incorporate photocatalysts with the

* Corresponding author.
E-mail addresses: Jaime.Fernandez-Pampillon@ciemat.es (J. Fernández-Pampillón), magdalena.palacios@ciemat.es (M. Palacios), lourdes.nunez@ciemat.es (L. Núñez), manuel.pujadas@ciemat.es (M. Pujadas).

https://doi.org/10.1016/j.cacint.2024.100170
Received 28 June 2024; Received in revised form 13 September 2024; Accepted 14 September 2024
Available online 21 September 2024

aim of reducing atmospheric pollution. In particular, the use of the semiconductor TiO_2 is becoming widespread due to its ability to accelerate the decomposition of atmospheric NO_x [6,7].

The absorption of UV-A light promotes the formation of electron-hole pairs in the conduction and valence bands that initiate the oxidation–reduction of various species adsorbed on the surface (oxygen, water) [8,9]. It leads to the formation of intermediate compounds of high reactivity that can decompose the adsorbed NO_x, which is converted into nitrate anions until it is washed away, e.g. by rain [10–13]. The mechanism of pollution decomposition is described elsewhere [14].

The research activity has been notable in recent decades, promoting the development of materials in which TiO_2 is a constituent of the coating that is deposited on the surface (e.g. glass, pavement, brick, etc.) or else it is embedded in the construction material itself (e.g. concrete). In many European cities, attempts have been made to take advantage of this technology in order to alleviate air pollution [21–23,15–20,24–27].

Certainly, the role that commercial photocatalytic materials can play in the air quality plans proposed by local governments needs to be studied in depth. NO_x removal efficiency of numerous TiO_2-based materials has been previously investigated at laboratory scale [10–13,28–35]. However, the range of photocatalytic products available on the market is very varied and abundant. And, best of our knowledge, no study has yet been conducted that has examined a large collection of commercial products intended for application on urban surfaces neither has selected the materials that are most suitable for use on these substrates.

On the other hand, there are relatively few studies that calculate NO_x surface deposition rates based on the removal efficiencies estimated in the laboratory, this parameter being crucial when modelling the impact that the implementation of this technology could have in an urban setting. In addition, the use of advanced numerical models is neither direct nor simple, and is not normally available to air quality managers. Simpler models are required that, using this parameter, allow the phenomenon of surface deposition of NO_x to be approximated.

This manuscript refers to various activities developed within the framework of the LIFE MINOx-STREET project ("Monitoring and modelling NO_x removal efficiency of photocatalytic materials: a strategy for urban air quality management") [36,37]. The main objective of the project was to evaluate whether the results of multiple laboratory tests and outdoor experiences evidenced the atmospheric NO_x purification capabilities of photocatalytic materials commonly marketed for urban applications. Some of the fundamental issues raised were: a) What is the range of NO_x removal efficiency of the commercially available photocatalytic materials?; b) What is the influence of environmental conditions on the most efficient materials?; c) What are their NO_x surface deposition rates?; d) What is the impact of the application of these materials in urban atmosphere?

This paper presents the methodology followed and the results obtained in relation to these questions. First, a number of standard tests was carried out, using a strict ISO testing protocol, in order to compare the potential urban functionality of photocatalytic materials as a nitrogen oxide sink. Second, the dependence with UV-A light, relative humidity and ambient pollutant concentrations of the NO_x purifying ability for the highest efficient products was analysed. Third, their respective NO surface deposition rates were estimated using two first-order kinetic modelling approaches. In addition, an estimate was made of what the NO_x sink effect could be by applying the selected materials in a street-canyon or, alternatively, using them in an urban device thought as an air purifier. Moreover, these scenarios have also been compared assuming a maximized NO_x removal capacity of such materials.

Methodology

In this section, the procedure used to compare NO_x-removal capability of photocatalytic materials is presented. Subsequently, the influence that some physical parameters may have on said efficiency has been analysed in a range of values usually observed in urban atmospheres. Finally, diverse kinetic approaches (first-order analysis and Langmuir–Hinshelwood model) used to estimate the NO surface deposition rates, that modellers need to evaluate the impact of this technology at urban scenarios, are described.

Photocatalytic NO_x activity of commercial materials on laboratory scale

Among the products that were available on the Spanish market, some were chosen whose characteristics were considered appropriate, after testing their NO air purification performance according to ISO 22197–1:2007, for putting them in place on roads, sidewalks and facades [38].

When TiO_2-based photocatalyst is not incorporated into the material, the way of application of the active products on different surfaces (by spraying, rolling, brushing), as well as a potential uneven distribution of the catalyst, could influence the NO removal efficiency [13,39,40]. Excepting of the paving blocks or slabs for sidewalks offered with the incorporated TiO_2-based photocatalyst, the rest of the tested samples were treated with active coatings following the manufacturers' instructions. A more in-depth analysis of the influence that those operating conditions may have on the measured photocatalytic activity really exceeds the objective of the present work.

NO removal experiments were carried out by the Department of Energy in CIEMAT. Succinctly, the experimental device used operates with a bed type-flow reactor consisting of a stainless-steel flat cell that houses the photocatalytic sample, with 100 mm (length) × 50 mm (wide) × 15 mm (depth) size. A borosilicate glass window covers the reactor, located 5 mm above the sample, allowing its illumination by means of 2 UV-A Phillips TL-8 W/05 fluorescent lamps, with a maximum emission at 365 nm wavelength, so that the irradiance on the surface of the tested material is 10 W/m^2 UV-A. A 100 ppm_v NO/N_2 gas cylinder was used to generate a mixture of test gases (NO, air, H_2O) (50% relative humidity −RH−) that is passed at 3 L/min rate over a rectangular photocatalytic sample. After stabilization of the required inlet NO concentration (1 ppm_v) under dark conditions (30 min), the quantity of NO_x that has been adsorbed by the test sample is determined. Afterwards, the photocatalytic surface is illuminated for 5 h. The photocatalytic material adsorbs and oxidizes NO to NO_2 as an intermediate of the photocatalytic reaction to, finally, form nitric acid (or nitrate). Under the experimental conditions described, reaction time is 0.5 s. During the test, the reactor inlet and outlet volume fractions of NO_x (ppm_v) are analysed and recorded (Signal Ambitech 447 chemiluminescence NO_x analyser), which makes it possible to determine the quantity of both NO and NO_x eliminated, and NO_2 formed. Finally, photo-irradiation is stopped and zero calibration gas is supplied at the same flow conditions (30 min). Then, the volumetric fraction of NO_x is recorded, allowing the quantity of NO_x that is desorbed from the test sample to be determined.

From these supplied data, firstly, the NO removed from the inlet gas and the NO_2 formed are calculated by means of the formulas:

$$NO(r) = (\phi/22.4)\int \left(C_{NO_{in}} - C_{NO_{out}}\right)dt \quad (1)$$

$$NO_2(f) = (\phi/22.4)\int \left(C_{NO_2}\right)dt \quad (2)$$

where $NO(r)$ and $NO_2(f)$ are the amount of NO removed and NO_2 formed (μmol), respectively. $C_{NO_{in}}$ is the inlet NO volume fraction (ppm_v) and $C_{NO_{out}}$ and C_{NO_2} are the NO and NO_2 volume fractions at exit of the reactor (ppm_v), respectively, and ϕ is the airflow rate (dry gas basis, 0 °C and 101.3 kPa) (L/min). The integration is taken over the time, in minutes, for which measurements are taken (5 h).

Next, the net amount of NO_x removed (μmol) can be expressed as:

$$NO_x(r) = NO_x(ads) + NO(r) - NO_2(f) - NO_x(des) \quad (3)$$

It is assumed that, in dark conditions, the total amounts of NO_x adsorbed, $NO_x(ads)$, and desorbed, $NO_x(des)$, by the photocatalytic sample are negligible.

The NO photocatalytic efficiency is frequently expressed as NO conversion, χ_{NO} (%). This is a percentage measure of the NO removal, formulated as:

$$\chi_{NO} = \left(\frac{C_{NO_{in}} - C_{NO_{out}}}{C_{NO_{in}}}\right)\cdot 100 \quad (4)$$

However, NO conversion is not the only factor that must be considered to evaluate the active material performance, since photocatalytic oxidation of NO involves a NO_2 generated as a reaction product that is not fully oxidized to nitrate ($C_{NO_{2out}}$) [41]. Therefore, the NO_2 formation, χ_{NO_2} (%), can be estimated by using:

$$\chi_{NO_2} = \left(\frac{C_{NO_{2out}}}{C_{NO_{in}}}\right)\cdot 100 \quad (5)$$

Moreover, NO_x conversion, χ_{NO_x} (%), must also be estimated, taking into account inlet and outlet NO_x concentrations, ($C_{NO_{xin}}$) and ($C_{NO_{xout}}$), respectively, as following:

$$\chi_{NO_x} = \left(\frac{C_{NO_{xin}} - C_{NO_{xout}}}{C_{NO_{xin}}}\right)\cdot 100 \quad (6)$$

Furthermore, another additional parameter, named nitrate selectivity, S (%), is used to calculate the percentage of removed NO that has been finally oxidized to harmless nitrate instead of toxic nitrogen dioxide and is obtained by using Eq. (7) [42].

$$S = \frac{NO_x(r)}{NO(r)}\cdot 100 \quad (7)$$

It should be noted that although the chosen photocatalytic product was remarkably efficient in terms of NO removal, significant quantities of NO_2 can be liberated into the atmosphere, and air quality, in terms of impact on human health, would be undoubtedly degraded rather than improved. Although European air quality regulations only set limit values for NO_2, the USA occupational health agencies OSHA, ACGIH and NIOSH set exposure limit values, assuming a Time-Weighted Average of 8 h per day and 40 h per week over the entire working life, at 25 ppm_v for NO and 1 to 3 ppm_v for NO_2 [43]. Although this relationship suggests that NO_2 is 8 to 25 times more toxic than NO, the reviewed studies use a much more conservative approximation, assuming that NO_2 contributes 3 times more than NO from the point of view of air toxicity [44–46]. Here, a $DeNO_x$ index (μmol), which points to toxicity of the outlet gas mixture from the photoreactor, based on that defined by other authors [44,47] is defined as:

$$DeNO_x = NO(r) - 3\cdot NO_2(f) \quad (8)$$

All these estimated parameters are then used for the ranking of the activity of the materials.

Influence of environmental parameters on NO photocatalytic activity

Among the previously photocatalytic materials assayed under the ISO 22197–1:2007, the three most promising were selected: a water dispersion for road bituminous mixture, a water dispersion for sidewalk concrete pavement and a covering for facade facing brick.

Afterwards, their NO photocatalytic activity was tested using the mentioned standard as a basis but modified in order to investigate how relevant operating parameters could determinate their performance (Table 1). UV-A illumination was set to 1 h.

Table 1
Experimental conditions of modified ISO 22197–1:2007 international standard test.

TARGET OPERATING CONDITIONS	VALUE
Flow rate (L/min)	3.0
Flow velocity above active surface (m/s)	0.2
Active surface (mm x mm)	50 x 100
Temperature (°C)	25
Inlet NO concentration (ppm_v)	0.14 to 1
Relative humidity (%)	20 to 85
Irradiance (300–400 nm) (W/m^2)	2 to 20

Estimation of NO deposition velocity on a photocatalytic surface

Nowadays, authors have defined the photocatalytic surface deposition velocity in diverse manners and no experimental method for its determination is universally established [48–53]. Taking as a starting point that NO efficiencies do not suffer mass transfer limitations, two alternative forms of analysis useful in order to estimate said parameter are presented.

Classical first-order kinetic analysis

It is commonly assumed that, when the ambient concentration of NO does not exceed 200 ppb_v, a first-order kinetic approximation can be used to describe its photocatalytic decomposition [33,54]. The first step of this analysis consists of estimating, from the experimental data, an activity coefficient (k_r) (s^{-1}), as follows:

$$k_r = -\frac{ln\left(C_{NO_{out}}/C_{NO_{in}}\right)}{t_r} \quad (9)$$

where t_r is the reaction time (s). However, k_r depends on the reactor design. To avoid this constraint, the use of an uptake coefficient, γ, has been proposed [55], which is defined as the proportion of collisions of the pollutant with the active surface leading to its adsorption and oxidation and expressed as:

$$\gamma_{NO} = \frac{4\cdot k_r}{\overline{v}\cdot a_V} \quad (10)$$

considering that a_V is the ratio between the photocatalytic surface and the volume of air over the test piece (m^{-1}) and $\overline{v}$ is the mean NO molecular velocity (m/s) calculated as:

$$\overline{v} = \sqrt{\frac{8\cdot R\cdot T}{\pi\cdot M}} \quad (11)$$

in whose definition the ideal gas constant (R) (J/(mol K)), the absolute temperature (T) (K) and the NO molar mass (M) (kg/mol) intervene. Afterwards, a photocatalytic surface deposition velocity ($V_{ph,NO}$) (m/s) can be obtained as following:

$$V_{ph,NO} = \frac{\gamma\cdot\overline{v}}{4} \quad (12)$$

In this manner, experimental data are used to estimate $V_{ph,NO}$, essential for modellers to compute deposition fluxes. In this work, an inlet NO concentration of approximately 0.14 ppm_v has been chosen to infer this parameter.

Langmuir–Hinshelwood kinetic model

Modelling of photocatalytic degradation of air pollutants, NO among them, is frequently approached using the Langmuir-Hinshelwood (LH) kinetic mechanism [30,56–61]. It is used here to derive a photocatalytic NO surface deposition velocity, $V_{ph,NO}$ [62].

The disappearance rate of NO reactant per unit surface area, r_{NO} (ppm_v m/s), is expressed in the LH mechanism as:

$$r_{NO} = \frac{kK_{ad}}{1 + K_{ad}C_{NO}} C_{NO} \quad (13)$$

where C_{NO} is the NO concentration (ppm_v), k is the reaction rate constant (ppm_v m/s) and K_{ad} is the adsorption equilibrium constant (ppm_v^{-1}), both kinetic parameters dependent on the temperature, irradiance, relative humidity and air pollutants level.

When steady-state is established, assuming a plug flow, the NO balance equation inside the reactor can be formulated as:

$$v_{air}\frac{dC_{NO}}{dx} = -a_V r_{NO} \quad (14)$$

where v_{air} is the air velocity along the sample surface (m/s).

The integration of Eq. (14), within the limits $C_{NO} = C_{NO_{in}}$ at x = 0 and $C_{NO} = C_{NO_{out}}$ at x = L (L, length of the active surface), gives:

$$\frac{ln\left(C_{NO_{in}}/C_{NO_{out}}\right)}{\left(C_{NO_{in}} - C_{NO_{out}}\right)} = kK_{ad}\frac{a_V L}{v_{air}\left(C_{NO_{in}} - C_{NO_{out}}\right)} - K_{ad} \quad (15)$$

By employing the Eq. (15) and experimental data under variable inlet NO concentration (in the 0.14 to 1 ppm_v range), k and K_{ad} are derived setting out $x = \frac{a_V L}{v_{air}\left(C_{NO_{in}} - C_{NO_{out}}\right)}$ versus $y = ln(C_{NO_{in}}/C_{NO_{out}})/(C_{NO_{in}} - C_{NO_{out}})$. The intercept is equal to $-K_{ad}$. Finally, the slope, kK_{ad}, represents $V_{ph.NO}$ (m/s), assuming that $K_{ad}C_{NO} \ll 1$ and, consequently, a first-order kinetics for the photocatalytic reaction is fulfilled.

NO_x purifying strength at different scales by using high-performance photocatalytic materials

Numerous laboratory studies show surface deposition rates of NO_2 similar to those estimated for NO for various TiO_2-based photocatalytic materials [33,51,62,63]. In this study, it has been assumed that the NO_x surface deposition velocities for each selected photocatalytic material are equal to the corresponding ones calculated for NO. Considering this fact, the removal of atmospheric NO_x has been modelled that would take place in two scenarios: (a) in a photocatalytic urban canyon (W x L x H = 38 m x 300 m x 16 m; and (b) in a photoactive purifying device (W x L x H = 0.3 m x 0.3 m x 3 m), equipped with forced ventilation, aimed to be used in an urban environment.

For both geometries, the system is treated as an ideal canyon with plug flow in which the air mass travels parallel to its longitudinal axis with a constant air speed [33,54]. Assuming first-order kinetics in the surface photocatalytic process (Eqs. (9)-(12)), the activity coefficient (k_r) and, subsequently, the NO_x removal efficiencies (χ_{NO_x}) can be estimated.

In addition, two alternatives for photocatalytic NO_x surface deposition have been considered: (1) the average of the estimated activity for the three selected materials was used ($5.6\ 10^{-3}$ m/s) and (2) an activity that allowed obtain a NO removal performance of 100% under ISO test conditions (0.1 m/s). Diverse air velocities ranges were also used for modelling: (a) under a common range of surface wind speeds in urban environments and (b) by using a helical extractor (0.3 m diameter and 150–1600 m^3/h flow rates). In Table 2, main physical and photocatalytic parameters used for modelling NO_x removal are shown.

For case (a), a maximum estimated NO_x photocatalytic potential was first calculated. It was subsequently corrected taking into account the possible real transport limitations by a factor of two [64] and that the urban canyon was illuminated by the sun only during the daytime period (12 h). In case (b), it was considered that the device has been designed to eliminate mass transport constraints and uses UV-A light lamps that allow continuous daily performance.

Table 2
Parameters used for modelling urban canyon and NO_x-purifier scenarios by using estimated or maximum $V_{ph.NO_x}$.

	Estimated $V_{ph.NO_x}$ ($5.6\ 10^{-3}$ m/s)		Maximum $V_{ph.NO_x}$ (0.1 m/s)	
	Urban canyon	NO_x-purifier	Urban canyon	NO_x-purifier
L (m)	300	3	300	3
Air velocity (m/s)	0.5–5	0.5–5	0.5–5	0.5–5
Active surface (m^2)	$2.1\ 10^4$	3.6	$2.1\ 10^4$	3.6
Volume (m^3)	$1.82\ 10^5$	0.27	$1.82\ 10^5$	0.27
a_V (m^{-1})	$1.15\ 10^{-1}$	13.3	$1.15\ 10^{-1}$	13.3
t_r (s)	600–60	6–1	600–60	6–1
k_r (s^{-1})	$6.45\ 10^{-4}$	$7.47\ 10^{-2}$	$1.15\ 10^{-2}$	1.33

Results

Comparison of the NO_x purification capacity of photocatalytic materials

The NO_x air-purifying ability of a notable diversity of commercial materials have been studied for their use on: road (bituminous mixture), sidewalk (concrete pavement) and facade (concrete pavement and facing brick) (see Table 3) (more details are given in Table S1). Further information are not described because confidentiality constraints imposed by manufacturers.

Fig. 1 shows estimates, based on the results of the tests carried out following standard ISO 22197–1:2007, for the quantity of NO removed, NO_x removed and NO_2 formed, related to the samples of the mentioned photocatalytic materials. A great variability from near non-active to highly active materials was found. The performance observed depends, in addition to the photoactive product, on several characteristics of the surface on which it is applied (e.g. the thickness, the porosity or the surface texture of the surface layer) [13,39,40,65–68].

An important aspect to take into account in the characterization of the NO_x purification capacity of a certain photocatalytic material is the conversion efficiency of the amount of oxidized NO_2 to nitrate. As it is displayed in Fig. 2, the NO conversion found for the active materials that have been tested does not correlate with their nitrate selectivity which implies that, even if NO is removed from the air mass in the reactor, a non-negligible amount of NO_2 is generated.

Three materials among those tested stand out for their high NO removal activity: $(BM\text{-}WD)_1$, $(PS\text{-}WD)_1$ and $(CS\text{-}FC)_1$, with efficiencies as outstanding as 65%, found for the sidewalk.

The heterogeneity of NO_x depolluting efficiency for road (35–9%), sidewalk (56–2%) and facade (28–2%) is shown in Fig. 3.

For the photocatalytic bituminous mixtures tested, ignoring the

Table 3
Nomenclature used for types of substrates and photocatalytic products studied.

NOMENCLATURE	
ROAD	
BM	bituminous mixture
CG	photocatalytic cement grout
WD	photocatalytic water dispersion
SIDEWALK	
PPB	paving block (integrated photocatalyst)
PPS	paving slab (integrated photocatalyst)
PS	paving slab
WD	photocatalytic water dispersion
FACADE	
CS	concrete surface
FB	facing brick
FC	photocatalytic facade covering

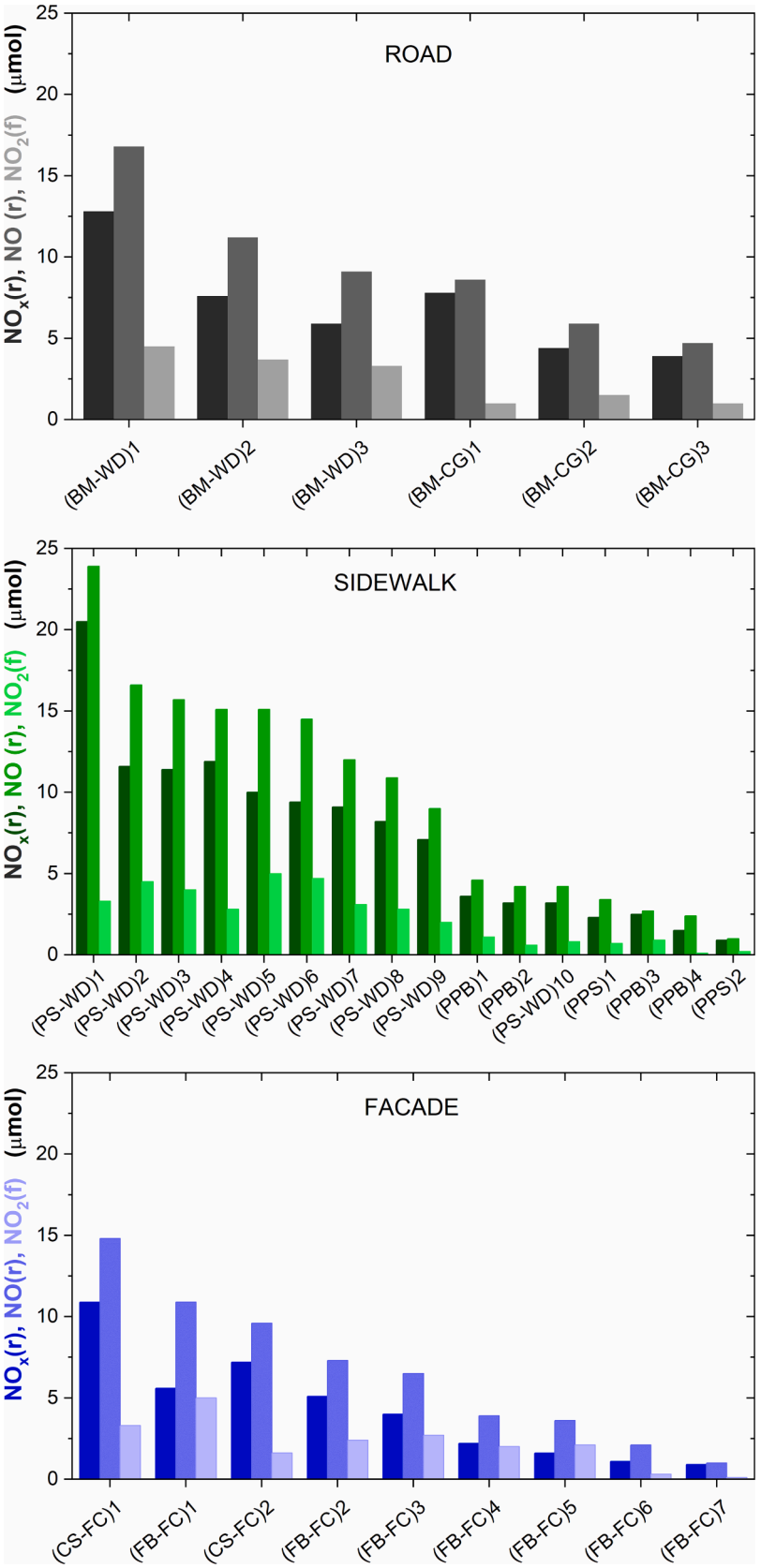

Fig. 1. NO_x removed, NO removed, NO_2 formed (µmol) of tested photocatalytic materials marketed for application on road, sidewalk and facade.

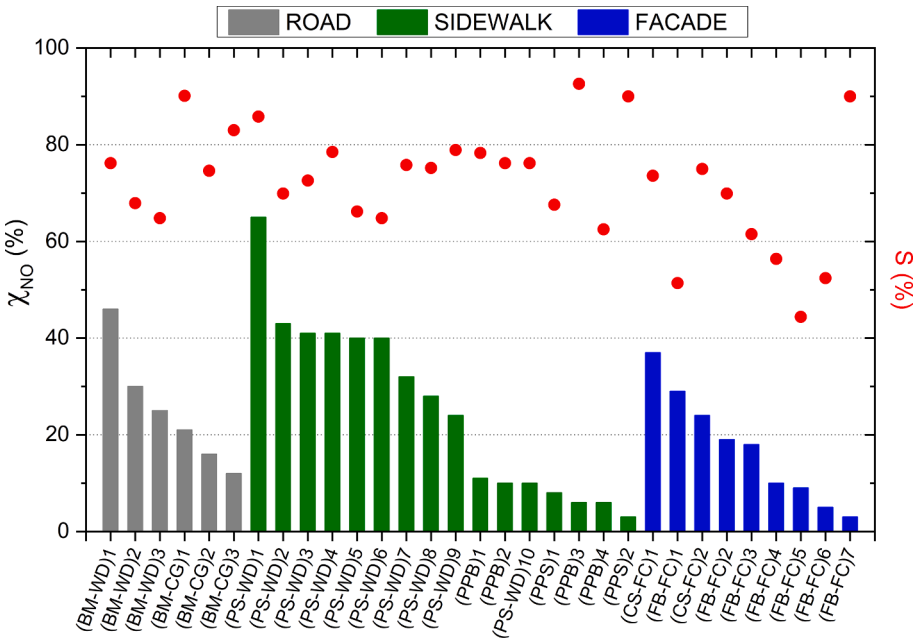

Fig. 2. NO photocatalytic efficiency (χ_{NO}) and selectivity (S) for tested photocatalytic products on diverse surfaces.

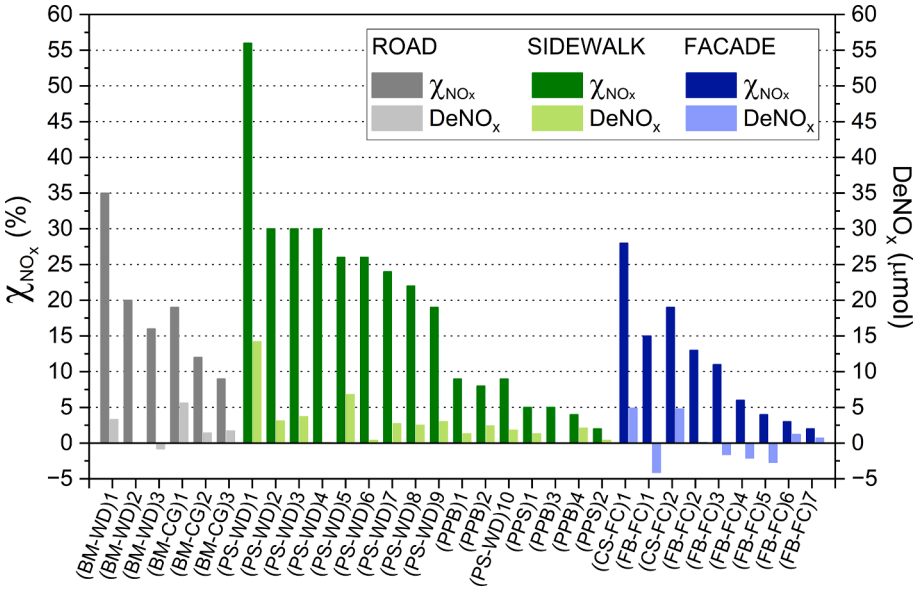

Fig. 3. NO_x removal capacity (χ_{NO_x}) and $DeNO_x$ index estimated for different photocatalytic materials tested for their potential applications on urban settings.

extreme values corresponding to the samples $(BM\text{-}WD)_1$ and $(BM\text{-}CG)_3$, the NO_x conversions found were between 12% and 20%. Furthermore, all samples presented a positive $DeNO_x$ index (0.1–5.6 μmol), except for $(BM\text{-}WD)_3$, for which it was negative (−0.8 μmol).

In relation to the photocatalytic pavements tested for implementation on sidewalks, the sample $(PS\text{-}WD)_1$ displays outstanding photocatalytic activity. Furthermore, two large groups of NO_x removal efficiency can be observed: one in which the values are in the range of 30% to 19%; and another in which the range extends from 9% to 2%. In no case was a negative $DeNO_x$ index (0–14 μmol) obtained.

Regarding the photocatalytic materials tested for application on the facade, those in which the highest NO_x conversion was observed were $(CS\text{-}FC)_1$ and $(CS\text{-}FC)_2$ (28% and 19%, respectively), whose substrate in both was the concrete. Its associated $DeNO_x$ index was approximately 5 μmol. Considering those photocatalytic materials whose substrate was facing brick, a NO_x removal performance of 15% to 2% and a negative $DeNO_x$ index was observed for nearly half of the samples tested, up to approximately −4 μmol, being of the order of 1 μmol for the rest.

In view of these results, the most appropriate materials were chosen to undertake the characterization of the influence that environmental variables exert on NO removal performance. For road and sidewalk application, $(BM\text{-}WD)_1$ and $(PS\text{-}WD)_1$ were chosen, respectively. For use in facades, although the photocatalytic samples with concrete substrate showed higher NO_x efficiencies and $DeNO_x$ indexes than those with facing brick as substrate, given the massive use of this last type of substrate in the municipality's facades in which photocatalytic materials were going to be implemented, those with a concrete substrate were excluded from the selection process. Furthermore, although samples $(FB\text{-}FC)_1$ and $(FB\text{-}FC)_2$ showed similar NO_x conversions, the $DeNO_x$ index of $(FB\text{-}FC)_1$ was notably negative, which would have led to the

choice of $(FB\text{-}FC)_2$. However, beyond the importance of photocatalytic efficiency, another crucial element to consider in practice is the acquisition cost of the material to be used (€/m^2). In this sense, the market price of $(FB\text{-}FC)_2$ was two and a half times higher than that of $(FB\text{-}FC)_1$, so the latter was finally selected.

Table S2 collects the NO_x photocatalytic performance provided by other authors, including basic information such as the selected photocatalytic material, the type of reactor used and the established test conditions. It offers a global and updated view, although not exhaustive, of the diversity of studies carried out on photocatalytic materials based on TiO_2 in which NO as inlet gas and flow-type reactors have been used.

Analysis of NO photocatalytic activity in response to environmental parameters

Once selected the photocatalytic materials for their implementation on roads, sidewalks and facades, $(BM\text{-}WD)_1$, $(PS\text{-}WD)_1$ and $(FB\text{-}FC)_1$, the influence of different variables ($C_{NO_{in}}$, UV-A irradiance and RH) on their NO removal performance was studied (Fig. 4).

The NO conversion appears to be unaffected even when the inlet NO concentration varies widely in the range of 0.14–1 ppm_v, in all cases studied (road, sidewalk and facade), as clearly shown in Fig. 4 (a). It is noteworthy that this occurs within the entire tested range of inlet NO concentration, that is, both for concentrations below 200 ppb, for which first-order kinetics can be assumed a priori, and for higher concentrations, for which, very frequently, the conversion decreases as the concentration of NO increases, the reaction order then being less than 1 [8]. NO_x conversion and selectivity follow the same trend described for NO, taking into account that not only the conversion of the latter does not depend on the inlet NO concentration, but also the formation of NO_2 is not affected, the latter being relatively small, of the order of 10%.

Regarding the dependence of NO_x removal on UV-A irradiance, when this parameter increases in a 2 to 10 W/m^2 range, a greater NO_x conversion is observed for all the samples analysed (Fig. 4 (b)). Above 10 W/m^2, higher performances of the photocatalytic materials are not achieved, tending the NO_x degradation curves to be asymptotic. It should be noted that the efficiency drops for values lower than 10 W/m^2 are more notable in the case of road and facade. Selectivity behaves accordingly and a non-zero NO_x removal is observed even under a low UV-A irradiance, except in the case of the facade sample, which reaches a nearly inactive state.

Regarding the degree of dependence of NO_x removal efficiency with different RH levels, all photocatalytic materials showed a non-linear diminishment of conversion when RH rises, with an abrupt lessening when the RH gets above 35%, in the cases of roadway and facade (Fig. 4 (c)). In the case of sidewalk, this inflection point is found at 50% RH. The values arrive to almost zero for figures between 60 and 85% RH, in all cases. In the case of the facade test, the conversions found for NO are significantly different from those obtained for NO_x, essentially due to a remarkable formation of NO_2.

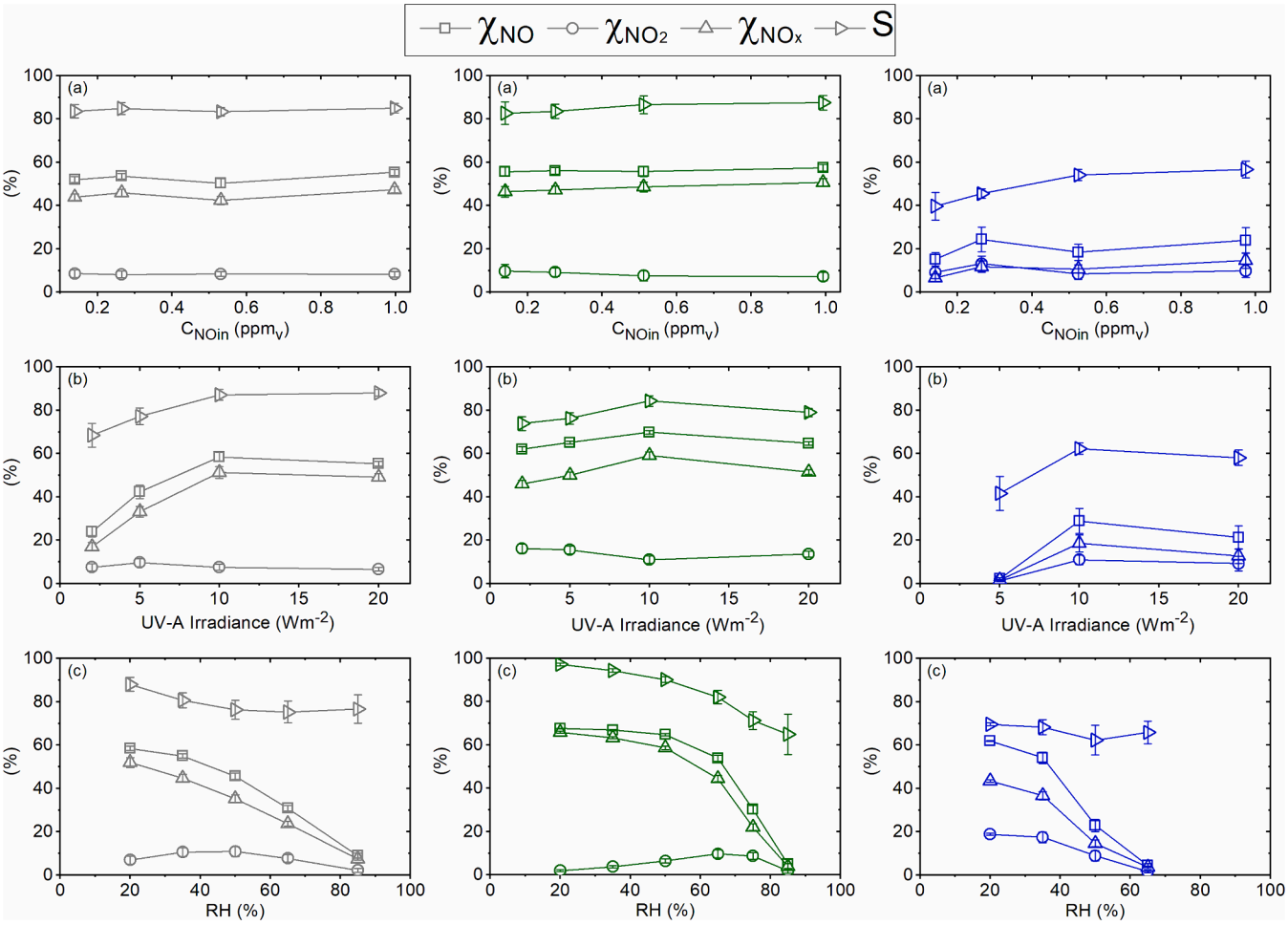

Fig. 4. Mean value and standard deviation for NO and NO_x conversions (χ_{NO} and χ_{NO_x}, respectively), NO_2 formation (χ_{NO_2}) and selectivity (S) of chosen materials for urban applications (road –grey–, sidewalk –green– and facade –blue–) as a function of different parameters: (a) $C_{NO_{in}}$, (b) UV-A irradiance and (c) RH. (For interpretation of the references to colour in this figure legend, the reader is referred to the web version of this article.)

Photocatalytic NO surface deposition velocities

NO conversions have been calculated for a wide range of inlet concentrations (0.14 to 1 ppm_v) for which the existence of first-order kinetics has been verified. Estimation of NO surface uptake and deposition velocity (according to Eqs. (9)-(12)) has been carried out in the range of ambient levels, 0.14 ppm_v NO, to which said kinetics is conventionally associated [33,54] (see Table 4).

On the other hand, as highlighted in Fig. 5, using the LH model and assuming that the slope of the linear regression gives the NO surface deposition velocity (according to Eq. (15), the estimated values for each selected material are: 7.4 10^{-3} m/s, 8.2 10^{-3} m/s and 1.5 10^{-3} m/s (road, sidewalk and facade, respectively).

Despite having used two different analysis methods, the surface deposition rates estimated for each selected active materials are very similar.

Analysis of NO_x purifying strength at different scales by using high-performance photocatalytic materials

The simulated atmospheric NO_x photocatalytic removal performance depends on the scenario geometry, the photocatalytic activity of the applied material and the air velocity (see Fig. 6).

When the NO_x surface deposition velocity is the average of those estimated under the ISO standard, the NO_x removal performance for the urban canyon and NO_x-purifier scenarios are very similar. In the range of velocities studied, from 0.5 to 5 m/s, they are reaching values of 32 to 4%, for the first scenario, and 36 to 4%, for the second, decreasing as the air velocity increases. However, when the limitations of mass transport and hours of solar irradiation in the urban canyon scenario are considered, the values decrease significantly (7 to 1%).

Moreover, if the NO_x surface deposition velocities were those necessary to achieve 100% NO_x removal performance under ISO conditions, the NO_x purification obtained, when there is no restriction either to transport or UV-A lighting in the urban canyon, is at significantly higher values (100 to 50%), being analogous to that achieved in the NO_x-purifier (100 to 55%). Under the somewhat more realistic hypothesis that the aforementioned limitations occurred in the urban canyon, performance would decrease significantly (22–11%).

Discussion

The information provided by manufacturers about their products sometimes includes some reference to the evaluation of atmospheric gas removal performance. However, a direct comparison of the results is not possible, as they could have been obtained using different testing procedures or standards. On the other hand, the substrate chosen for the application of said products will determine to a large extent, as it has been already mentioned, the effectiveness obtained.

In this work, a miscellany of commercial photoactive products and substrates frequently available in the Spanish market has been tested to assess their air purifying ability in order to select the most promising ones (Table S1). There is no universal standardized test and strengths and weaknesses of experimental set-ups are on continuous review [54,69–71]. Here, the ISO 22197–1:2007–1 standard, available in CIEMAT, and well known and widely utilized in numerous scientific studies, has been used as the unique standard in order to ensure that the internal coherence of the comparison made is as great as possible.

Additionally, in order to contextualize the NO and NO_x efficiencies found in this study, a broad but not exhaustive bibliographic review of related works has been carried out, collected in the Table S2. A wide range of results obtained is evident depending on test conditions. Some of those experiences, developed under the usual testing conditions of the ISO standard, have been included, as well as some others that take it as a reference but apply it with certain modifications. Furthermore, other authors have carried out studies of NO conversion efficiencies on different photocatalytic materials using other standards and reactor geometries, in which the flow conditions are necessarily different and the photocatalytic activity is consequently affected.

When the flow established in an ISO bed flow photo-reactor is laminar, the transport of the gas to the surface is limited in fast heterogeneous reactions and vertical concentration gradients are present. This implies an underestimation of the actual kinetics, which becomes significant with uptake coefficients greater than 10^{-5} [30,54].

To overcome the diffusion restriction in ISO tests, several authors have proposed different solutions. For example, the introduction of physical barriers that induce turbulent mixing in the reactor and prevent the appearance of vertical concentration gradients on the active surface [54]. Other authors who have not modified the ISO reactor geometry have promoted turbulent mixing using non-planar carrier materials, so that the flow exclusively presents a concentration gradient in the direction of gas advance [33]. Finally, several studies have used different suitable reactor geometries to eliminate the mass transfer limitations [39,51,58,69,72–75]. The lack of mass transfer constraints allows to approximate the kinetics with a first-order formulation and an ideal plug-flow model can be applied [76].

In this study, photocatalytic materials assayed show quite different textures. Bituminous mixtures samples, within a 0.6 to 2.2 mm range (Centre for Studies and Experimentation of Public Works CEDEX, Spain) (personal communication); sidewalk samples tested present Concrete Surface Profiles (CSP), following the standard developed by the International Concrete Repair Institute [77], from CSP-4 to CSP-8; and facade samples exhibit CSP-3 and CSP-8 profiles. The rough surface of photocatalytic samples, together with the short residence time imposed in the ISO test, cooperate to induce a homogeneous vertical distribution of the concentration of gaseous pollutant [33,54]. Thanks to this, it has been possible to carry out a comparison of the photocatalytic ability for NO_x removal of a broad assortment of products offered for their urban implementation and, subsequently, establish a ranking that would allow a reasonable choice for each type of application (road, sidewalk or facade).

Even more, for the three different photocatalytic materials that have been finally selected, different inlet concentrations of NO have been used (0.14 to 1 ppm_v) and similar values of χ_{NO} have been obtained, verifying a first-order kinetic behaviour [54,78]. Most of the reviewed authors have observed an inverse dependence of the estimated NO_x conversion with inlet NO concentration within the 0.025–2 ppm_v range (Table S2), which implies a deviation from first order kinetics. However, in the same test interval, some studies showed a positive linear correlation between the NO levels at the inlet and outlet of the reactor. That means the NO reaction rate constant and, consequently, the associated uptake coefficient, did not suffer any change when altering the initial NO concentration, verifying a first order kinetics [10,12,78].

The three materials selected for urban application showed a directly proportional relationship between UV-A irradiance and NO_x degradation efficiency, the latter remaining constant at values above 10 W/m^2. Most of the studies analysed that have assessed this dependence worked in a similar variable range (Table S2). As the irradiance raises, the amount of surface TiO_2-active sites available on the photocatalytic material enlargers, redox reactions accelerate and, consequently, the NO_x removal efficiency grows up. However, the number of those is

Table 4
Estimated NO uptake coefficients and surface deposition velocities (mean and standard deviation) for the selected materials from a first-order analysis carried out under the following conditions: $C_{NO_{in}} \sim 140$ ppb_v, UV-A irradiance = 10 W/m^2, RH = 50% and $\phi = 3$ L/min.

	$C_{in,NO}$ (ppb_v)	γ_{NO} (10^{-5})	$V_{ph,NO}$ (10^{-3}) (m/s)
ROAD	139 ± 2	6.5 ± 0.3	7.2 ± 0.5
SIDEWALK	140 ± 4	7.2 ± 0.4	8.0 ± 0.5
FACADE	141 ± 3	1.5 ± 0.3	1.6 ± 0.4

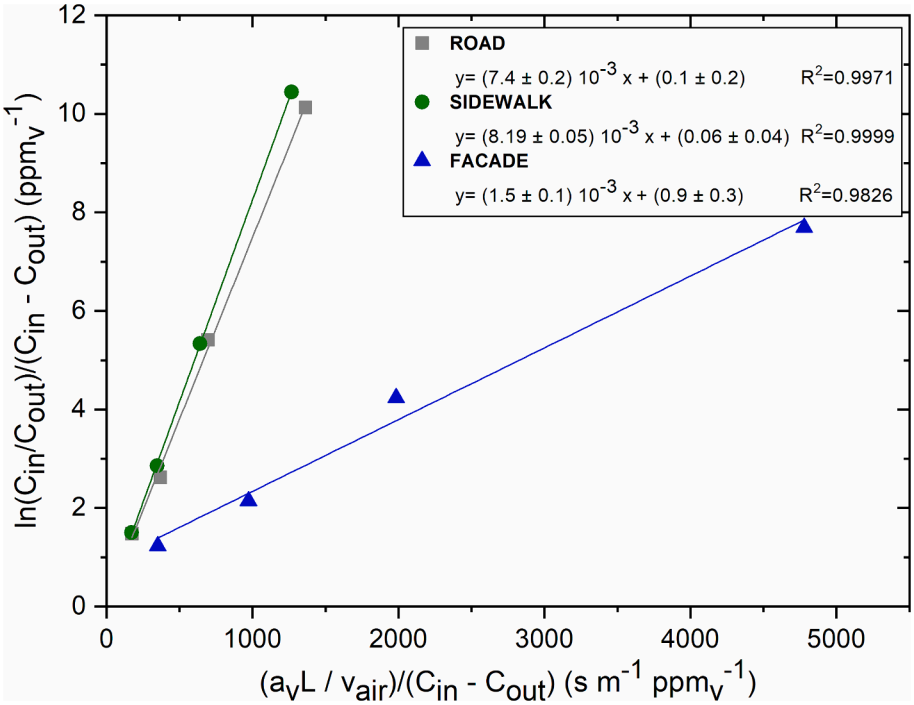

Fig. 5. Linear fit from NO photocatalytic decomposition data on road, sidewalk and facade selected samples by using the LH kinetic approximation.

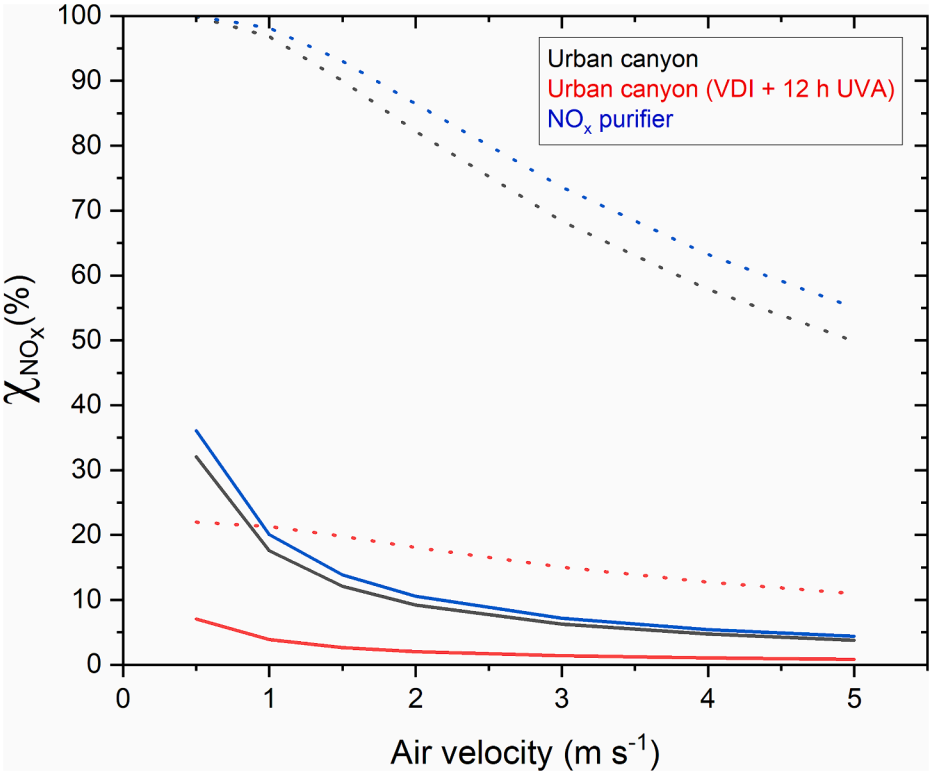

Fig. 6. χ_{NO_x} as a function of air velocity, for urban canyon and NO_x-purifier scenarios. Solid lines refer to estimated $V_{ph.NO_x}$ (5.6 10^{-3} m/s) and dashed lines, to maximum $V_{ph.NO_x}$ (0.1 m/s).

limited and, above a certain threshold, a greater light intensity does not improve the performance [8,10,34,39,78–81]. This seems to be a common behaviour in photoactivated processes and corresponds with two different states: first-order or half-order, depending on whether the consumption of the electron-hole pairs is fundamentally determined by the photooxidation or recombination process, respectively [82].

In addition, other authors have expanded the range of assay up to nearly 50 W/m^2 establishing that at 10–20 W/m^2, a maximum value is reached, constant up to the upper limit tested [31,33]. Therefore, UV-A radiation causes an increase in the NO_x degradation curves that tend to

be asymptotic. However, other authors that have extended the scope up to 40–80 W/m^2, also finding a positive correlation of uptake with irradiance though not asymptotic [83,84].

Regarding the repercussion of relative humidity on the NO_x photocatalytic oxidation capacity, the reviewed authors have worked within various ranges of RH values (Table S2). Most of these studies have evidenced a negative relationship between NO_x conversion and relative humidity throughout the study interval [28–30,33,38,40,57,72,81–85], even becoming more noticeable at high relative humidity [33]). Besides, some authors have informed that oxidising activity did not change noticeably until a certain humidity level was reached and then decreased [10,84]; and other studies have documented a growth in NO_x degradation with increasing relative humidity until an inflection point in which an opposite or constant trend was established [13,56,79,81]. Finally, some research has not found a significant influence of RH on NO_x degradation [13,84].

The dependence of the photocatalytic reaction on humidity is complex, and diverse behaviours can be observed depending on both the photocatalytic materials tested and the conditions imposed on the experiment. When humidity levels are low, the interaction of H_2O molecules with the active surface is the limiting factor of photocatalytic reaction to take place, since it controls the formation of hydroxyl radicals necessary for the oxidation of NO (oxidizing effect). On contrast, at high relative humidity, the inverse behaviour of photocatalytic efficiency and relative humidity is generally associated to the affinity of the H_2O, NO and NO_2 molecules for the same TiO_2 centres. The access of the target pollutants to active sites is more difficult, resulting in a low effective NO oxidation (hydrophilic effect).

Regarding the behaviour of nitrate selectivity in response to variation in system parameters, most of the published studies reviewed (Table S2) show results similar to those described in this work. When responses to changes in inlet NO concentration are analysed, this parameter remains constant up to 1 ppm_v, decreasing significantly above this concentration [41]. The selectivity also remains nearly constant in a range of clearly higher NO concentrations (5 to 60 ppm_v) [56]. In relation to the influence that an increase in UV-A irradiance may have on nitrate selectivity, the study analysed [56] shows a clear growth at NO concentrations of 5 ppm_v. When concentrations are much higher, no effect is observed. Finally, an increase in relative humidity causes a clear decrease in nitrate selectivity [41,86] although, alternatively, at much higher NO concentrations (40 ppm_v) changes in relative humidity do not seem to have any impact [56].

For the selected photocatalytic samples, it has been verified that the experimental system operates as a plug flow reactor in which there are no diffusion limitations or, in other words, that the photooxidation process is not controlled by the transport of the gas molecules downward to the test sample and, consequently, can be described by a first-order kinetic law.

Under mentioned conditions, two kinetic approaches have been used in order to calculate $V_{ph,NO}$, a classical first-order kinetic analysis and the LH model. The estimated values for each type of urban use were very similar for both, from 2 to 8 10^{-3} m/s, although the first is notably simpler at experimental and calculation levels than the latter. Other authors have calculated values of surface deposition rates of NO and NO_2, for different photocatalytic materials, by using an experimental set-up based on ISO, and applying the aforementioned analysis methods, obtaining values in most cases of the same order of magnitude (Table S3). On the other side, NO_2 surface deposition rates have not been estimated in the present work. However, studies in which the photocatalytic elimination of NO_2 has been tested under laboratory conditions, offered values of surface deposition rates for this contaminant that are very similar to those reported for NO, equal to or an order of magnitude smaller (Table S3). These surface deposition velocities for NO_x pollutants serve the purpose of calculating what the removal of ambient NO_x could be in a real urban scenario, as required by atmospheric dispersion models.

The removal efficiency of atmospheric NO_x using photocatalytic materials on urban surfaces is limited in practice by several factors. The first of them is the capacity of the material used. In this sense, current research focuses on the development of increasingly efficient TiO_2-based materials, some of them with very notable NO_x surface deposition rates of the order of 30 10^{-3} m/s (Table S3). However, the substrates used are not those commonly applied in urban environments and the values obtained are still far from those calculated to achieve maximum ideal NO_x removal performance. Another factor to take into account is the complex conditions of turbulent mixing in the urban canyon, conditioned by wind flows and street geometry, which can impose even greater restrictions on transportation than those estimated. Furthermore, the wind speed and the active surface area to volume ratio will influence efficiency, with this decreasing the greater the intensity of the wind and the narrower the urban canyon. On the other hand, UV-A lighting can be reduced much during the daytime period compared to the proposed one (12 h), depending on the orientation of the street and the shadows cast. Finally, without attempting an exhaustive list, it might be noted that the truly active surface on the street is obviously less than that available (traffic on the road, parked vehicles, windows on the facades, etc.).

There is, however, the alternative of using the NO_x purification capacity of these materials using devices that increase the ratio of active surface area to volume of treated air and regulate the airflow through them as appropriate. These elements can have interior mesh that further increases the active surface and have UV-A lamps inside that ensure uninterrupted photocatalytic activity. The design of these purifiers can be adapted to the needs of the environment that is intended to be purified [63,88], resulting in a feasible proposal that could contribute to improving the quality of local urban air.

Conclusion

A robust testing methodology is mandatory to ensure the appropriate choice of products capable of removing NO_x from ambient air, considering the applications projected on a real scale, among all those offered as potentially successful. Numerous usable options in the Spanish market have been evaluated and compared. For that aim, a standard ISO test has been chosen. The results point out that the achievement in NO_x purification is determined both by the way in which the TiO_2-photocatalyst is integrated into a product and by the surface on which it is applied, which entails a high degree of disparity in the results obtained. Not all products tested under ISO 22197–1:2007 assay have shown significant photocatalytic activity but some of them have demonstrated a substantial capacity to remove NO_x (>10%).

The appropriate range of different physical parameters, UV-A irradiance, inlet NO concentration and relative humidity, necessary to guarantee the photocatalytic NO_x removal competence of the three materials elected for application in an urban environment has been determined. The dependence of the performance on these variables presents a general trend very similar to that found by the majority of the authors consulted, except for the concentration of the gas-phase pollutant. For this parameter, a constant value has been observed in a range of values up to 1 ppm_v, which has made it possible to verify the establishment of a first-order kinetic regime.

Taking mentioned ISO standard as a basis, but using an inlet NO concentration of 140 ppb_v, two different numerical approaches have been utilised to infer NO surface deposition velocities for the selected photoactive materials, to be applied on different urban surfaces, adjusting the degradation rate to a first order kinetics, arriving both methods to very similar results. Furthermore, although this standard has not been implemented to infer any NO_2 surface deposition rate, available studies revised have yielded values similar to those associated to NO, being the same magnitude or an order smaller. These estimates are crucial in numerical simulations to figure out the foreseen impact of this technology in urban atmosphere and evaluate its use in relation to air quality policy planning.

The NO_x removal efficiency of different selected commercial photocatalytic materials has been simulated, using a first-order kinetic approach, under different environmental conditions, in two scenarios (an urban canyon and a purifying device). The improvement of urban air quality is limited when these products are applied to urban canyon surfaces, but this type of materials could be used in air cleaning devices although before installation a larger-scale modelling is needed to confirm that alleviate local NO_x atmospheric pollution.

CRediT authorship contribution statement

J. Fernández-Pampillón: Writing – review & editing, Writing – original draft, Project administration, Methodology, Investigation, Funding acquisition, Formal analysis, Data curation, Conceptualization. **M. Palacios:** Writing – review & editing, Writing – original draft, Project administration, Methodology, Investigation, Funding acquisition, Formal analysis, Data curation, Conceptualization. **L. Núñez:** Writing – review & editing, Writing – original draft, Visualization, Methodology, Investigation, Formal analysis, Data curation, Conceptualization. **M. Pujadas:** Writing – review & editing, Writing – original draft, Supervision, Methodology, Investigation, Formal analysis, Conceptualization.

Declaration of competing interest

The authors declare that they have no known competing financial interests or personal relationships that could have appeared to influence the work reported in this paper.

Data availability

Data will be made available on request.

Acknowledgments

This study has been developed in the context of the LIFE MINOx-STREET project (LIFE12 ENV/ES/000280), co-funded by European Commission. We largely appreciate our colleagues from the Energy Department of CIEMAT (Spain), involved in ISO 22197-1:2007 laboratory tests.

Appendix A. Supplementary material

Supplementary data to this article can be found online at https://doi.org/10.1016/j.cacint.2024.100170.

References

[1] European Environment Agency. Air Quality in Europe 2022. 2022. https://doi.org/10.2800/488115.
[2] European Commission. Towards Zero Pollution for Air, Water and Soil. 2021. https://eur-lex.europa.eu/legal-content/EN/TXT/?uri=CELEX%3A52021DC0400.
[3] World Health Organization . WHO global air quality guidelines: particulate matter (PM2.5 and PM10), ozone, nitrogen dioxide, sulfur dioxide and carbon monoxide. 2021. https://www.who.int/publications/i/item/9789240034228.
[4] European Parliament and Council of the EU. Directive 2008/50/EC on ambient air quality and cleaner air for Europe. Off J Eur Union 2008. https://eur-lex.europa.eu/legal-content/ES/TXT/?uri=celex%3A32008L0050.
[5] Environmental Protection Agency. Nitrogen Dioxide (NO2) Pollution. 2023. https://www.epa.gov/no2-pollution/basic-information-about-no2#Effects.
[6] Chen H, Nanayakkara CE, Grassian VH. Titanium dioxide photocatalysis in atmospheric chemistry. Chem Rev 2012;112:5919–48. https://doi.org/10.1021/cr3002092.
[7] Fujishima A, Zhang X. Titanium dioxide photocatalysis: present situation and future approaches. Comptes Rendus Chim 2006;9:750–60. https://doi.org/10.1016/j.crci.2005.02.055.
[8] Herrmann J-M. Photocatalysis fundamentals revisited to avoid several misconceptions. Appl Catal B Environ 2010;99:461–8. https://doi.org/10.1016/j.apcatb.2010.05.012.
[9] Hoffmann MR, Martin ST, Choi W, Bahnemann DW. Environmental applications of semiconductor photocatalysis. Chem Rev 1995;95:69–96. https://doi.org/10.1021/cr00033a004.
[10] Bengtsson N, Castellote M. Photocatalytic activity for NO degradation by construction materials: parametric study andmultivariable correlations. J Adv Oxid Technol 2010;13:341–9. https://doi.org/10.1515/jaots-2010-0311.
[11] Karapati S, Giannakopoulou T, Todorova N, Boukos N, Antiohos S, Papageorgiou D, et al. TiO2 functionalization for efficient NOx removal in photoactive cement. Appl Surf Sci 2014;319:29–36. https://doi.org/10.1016/j.apsusc.2014.07.162.
[12] Laufs S, Burgeth G, Duttlinger W, Kurtenbach R, Maban M, Thomas C, et al. Conversion of nitrogen oxides on commercial photocatalytic dispersion paints. Atmos Environ 2010;44:2341–9. https://doi.org/10.1016/j.atmosenv.2010.03.038.
[13] Martinez T, Bertron A, Ringot E, Escadeillas G. Degradation of NO using photocatalytic coatings applied to different substrates. Build Environ 2011;46:1808–16. https://doi.org/10.1016/j.buildenv.2011.03.001.
[14] Chen J, Poon C. Photocatalytic construction and building materials: from fundamentals to applications. Build Environ 2009;44:1899–906. https://doi.org/10.1016/j.buildenv.2009.01.002.
[15] Ballari MM, Brouwers HJH. Full scale demonstration of air-purifying pavement. J Hazard Mater 2013;254–255:406–14. https://doi.org/10.1016/j.jhazmat.2013.02.012.
[16] Barratt, B., Carslaw, D., Green, D., 2012. High Holborn D-NOx Paint Trial – Report 3 (Updated).
[17] Boonen E, Beeldens A. Recent photocatalytic applications for air purification in Belgium. Coatings 2014;4:553–73. https://doi.org/10.3390/coatings4030553.
[18] Chen M, Chu JW. NOx photocatalytic degradation on active concrete road surface - from experiment to real-scale application. J Clean Prod 2011;19:1266–72. https://doi.org/10.1016/j.jclepro.2011.03.001.
[19] Cordero JM, Hingorani R, Jimenez-Relinque E, Grande M, Cutillas F, Martinez E, et al. Challenges in quantification of photocatalytic NO_2 abatement effectiveness under real world exposure conditions illustrated by a case study. Sci Total Environ 2021;766:144393. https://doi.org/10.1016/j.scitotenv.2020.144393.
[20] Fernández-Pampillón J, Palacios M, Núñez L, Pujadas M, Sanchez B, Santiago JL, et al. NOx depolluting performance of photocatalytic materials in an urban area – Part I: monitoring ambient impact. Atmos Environ 2021;251:118190. https://doi.org/10.1016/j.atmosenv.2021.118190.
[21] Gallus M, Akylas V, Barmpas F, Beeldens A, Boonen E, Boréave A, et al. Photocatalytic de-pollution in the Leopold II tunnel in Brussels: NOx abatement results. Build Environ 2015;84:125–33. https://doi.org/10.1016/j.buildenv.2014.10.032.
[22] Gallus M, Ciuraru R, Mothes F, Akylas V, Barmpas F, Beeldens A, et al. Photocatalytic abatement results from a model street canyon. Environ Sci Pollut Res 2015;22:18185–96. https://doi.org/10.1007/s11356-015-4926-4.
[23] Guerrini GI, Peccati E. Photocatalytic cementitious roads for depollution. In: Casssar PB, Cassar L, editors. International RILEM Symposium on Photocatalysis, Environment and Construction Materials. RILEM Publications SARL; 2007. p. 179–86.
[24] IPL, 2010. Dutch Air Quality Innovation Programme concluded. Improved Air Quality with Coating of Titanium Dioxide not Demonstrated.
[25] Maggos T, Plassais A, Bartzis JG, Vasilakos C, Moussiopoulos N, Bonafous L. Photocatalytic degradation of NOx in a pilot street canyon configuration using TiO_2-mortar panels. Environ Monit Assess 2008;136:35–44. https://doi.org/10.1007/s10661-007-9722-2.
[26] Moussiopoulos N, Barmpas P, Ossanlis I, Bartzis J. Comparison of numerical and experimental results for the evaluation of the depollution effectiveness of photocatalytic coverings in street canyons. Environ Model Assess 2008;13:357–68. https://doi.org/10.1007/s10666-007-9098-2.
[27] Tera Environment.. In Situ Study of the Air Pollution Mitigating Properties of Photocatalytic Coating. Report 09-RD-123. 2009. https://www.atmo-auvergnerhonealpes.fr/publications/eco-coating-etude-situ-des-proprietes-purificatrices-de-revetements-photocatalytiques.
[28] Ângelo J, Andrade L, Mendes A. Highly active photocatalytic paint for NOx abatement under real-outdoor conditions. Appl Catal A 2014;484:17–25. https://doi.org/10.1016/j.apcata.2014.07.005.
[29] Ballari MM, Hunger M, Hüsken G, Brouwers HJH. Modelling and experimental study of the NOx photocatalytic degradation employing concrete pavement with titanium dioxide. Catal Today 2010;151:71–6. https://doi.org/10.1016/j.cattod.2010.03.042.
[30] Ballari MM, Hunger M, Hüsken G, Brouwers HJH. NOx photocatalytic degradation employing concrete pavement containing titanium dioxide. Appl Catal B Environ 2010;95:245–54. https://doi.org/10.1016/j.apcatb.2010.01.002.
[31] de Melo JVS, Trichès G. Evaluation of the influence of environmental conditions on the efficiency of photocatalytic coatings in the degradation of nitrogen oxides (NOx). Build Environ 2012;49:117–23. https://doi.org/10.1016/j.buildenv.2011.09.016.
[32] Mendoza C, Valle A, Castellote M, Bahamonde A, Faraldos M. TiO_2 and TiO_2–SiO_2 coated cement: comparison of mechanic and photocatalytic properties. Appl Catal B Environ 2015;178:155–64. https://doi.org/10.1016/j.apcatb.2014.09.079.
[33] Mothes F, Ifang S, Gallus M, Golly B, Boréave A, Kurtenbach R, et al. Bed flow photoreactor experiments to assess the photocatalytic nitrogen oxides abatement under simulated atmospheric conditions. Appl Catal B Environ 2018;231:161–72. https://doi.org/10.1016/j.apcatb.2018.03.010.
[34] Sikkema JK, Ong SK, Alleman JE. Photocatalytic concrete pavements: Laboratory investigation of NO oxidation rate under varied environmental conditions. Constr Build Mater 2015;100:305–14. https://doi.org/10.1016/j.conbuildmat.2015.10.005.

[35] Zouzelka R, Rathousky J. Photocatalytic abatement of NOx pollutants in the air using commercial functional coating with porous morphology. Appl Catal B Environ 2017;217:466–76. https://doi.org/10.1016/j.apcatb.2017.06.009.
[36] European Commission. MonItoring and modelling NOx removal efficiency of photocatalytic materials: A STRategy for urban air quality managEmEnT.. https://webgate.ec.europa.eu/life/publicWebsite/index.cfm?fuseaction=search.dspPage&n_proj_id=4673.
[37] Palacios M, Núñez L, Pujadas M, Fernández-Pampillón J, Fernández JM, Sanchez BS, et al. LIFE MINOx-STREET Project. FuturENVIRO 2018;50:93–6. http://documenta.ciemat.es/handle/123456789/3440.
[38] ISO. Fine ceramics (advanced ceramics, advanced technical ceramics) — Test method for air-purification performance of semiconducting photocatalytic materials — Part 1: Removal of nitric oxide. ISO 22197-1 : 2007.2007. https://www.iso.org/standard/65416.html.
[39] Hüsken G, Hunger M, Brouwers HJH. Experimental study of photocatalytic concrete products for air purification. Build Environ 2009;44:2463–74. https://doi.org/10.1016/j.buildenv.2009.04.010.
[40] Jiménez-Relinque E, Hingorani R, Rubiano F, Grande M, Castillo Á, Castellote M. In situ evaluation of the NOx removal efficiency of photocatalytic pavements: statistical analysis of the relevance of exposure time and environmental variables. Environ Sci Pollut Res 2019;26:36088–95. https://doi.org/10.1007/s11356-019-04322-y.
[41] Si H, Zhou M, Fang Y, He J, Yang L, Wang F. Photocatalytic concrete for NOx degradation: influence factors and durability. Constr Build Mater 2021;298:123835. https://doi.org/10.1016/j.conbuildmat.2021.123835.
[42] Ângelo J, Andrade L, Madeira LM, Mendes A. An overview of photocatalysis phenomena applied to NOx abatement. J Environ Manage 2013;129:522–39. https://doi.org/10.1016/j.jenvman.2013.08.006.
[43] Lewis RJ, Sax NI. Sax's Dangerous Properties of Industrial Materials. 9th ed. Van Nostrand Reinhold; 1996. https://archive.org/details/saxsdangerouspro0000lewi/page/n5/mode/2up.
[44] Bloh JZ, Folli A, Macphee DE. Photocatalytic NOx abatement: why the selectivity matters. RSC Adv 2014;4:45726–34. https://doi.org/10.1039/C4RA07916G.
[45] Russell HS, Frederickson LB, Hertel O, Ellermann T, Jensen SS. A review of photocatalytic materials for Urban NOx remediation. Catalysts 2021. https://doi.org/10.3390/catal11060675.
[46] Serpone N. Heterogeneous photocatalysis and prospects of TiO_2-based photocatalytic DeNOxing the atmospheric environment. Catalysts 2018;8:553. https://doi.org/10.3390/catal8110553.
[47] Binetti Basterrechea GF, Montesinos VN, Quici N. Photocatalytic NOx removal with TiO_2-impregnated 3D-printed PET supports. Heliyon 2023;9:e22635. https://doi.org/10.1016/j.heliyon.2023.e22635.
[48] Kontos AG, Katsanaki A, Likodimos V, Maggos T, Kim D, Vasilakos C, et al. Continuous flow photocatalytic oxidation of nitrogen oxides over anodized nanotubular titania films. Chem Eng J 2012;179:151–7. https://doi.org/10.1016/j.cej.2011.10.072.
[49] Maggos T, Bartzis JG, Leva P, Kotzias D. Application of photocatalytic technology for NOx removal. Appl Phys A 2007;89:81–4. https://doi.org/10.1007/s00339-007-4033-6.
[50] Maggos T, Bartzis JG, Liakou M, Gobin C. Photocatalytic degradation of NOx gases using TiO_2-containing paint: a real scale study. J Hazard Mater 2007;146:668–73. https://doi.org/10.1016/j.jhazmat.2007.04.079.
[51] Mikyskova E, Martiniakova I, Zouzelka R, Rathousky J. Photocatalytic NOx abatement: the effect of high air flow velocity. Environ Technol Innov 2022;28:102820. https://doi.org/10.1016/j.eti.2022.102820.
[52] Soergel C, Burgeth G, Duttlinger W, Maban M, Kleffmann J, Flassak T. Numerische Modellierung des photokatalytischen Stickoxidabbaus durch TiO_2-dotierte Gebaudefassaden. Kolloquium Luftqualitaet an Strassen. FGSV Verlag; 2011. https://trid.trb.org/View/1125432.
[53] Tang X, Ughetta L, Gould RAT, Everman RLA, Skorina T, Chen S, Kavanagh M, Levinson R, Destaillats H. Pilot-scale NOx removal efficacy of photocatalytic roofing granules under urban environmental conditions. Sol. Energy Mater. Sol. Cells 2022;247:111907. https://doi.org/10.1016/j.solmat.2022.111907.
[54] Ifang S, Gallus M, Liedtke S, Kurtenbach R, Wiesen P, Kleffmann J. Standardization methods for testing photo-catalytic air remediation materials: problems and solution. Atmos Environ 2014;91:154–61. https://doi.org/10.1016/j.atmosenv.2014.04.001.
[55] Finlayson-Pitts BJ, Pitts Jr JN. Chemistry of the Upper and Lower Atmosphere. Academic Press; 2000.
[56] Devahasdin S, Fan C, Li K, Chen DH. TiO_2 photocatalytic oxidation of nitric oxide: transient behavior and reaction kinetics. J Photochem Photobiol A Chem 2003;156:161–70. https://doi.org/10.1016/S1010-6030(03)00005-4.
[57] Dong Y, Bai Z, Liu R, Zhu T. Decomposition of indoor ammonia with TiO_2-loaded cotton woven fabrics prepared by different textile finishing methods. Atmos Environ 2007;41:3182–92. https://doi.org/10.1016/j.atmosenv.2006.08.056.
[58] Hunger M, Hüsken G, Brouwers HJH. Photocatalytic degradation of air pollutants - From modeling to large scale application. Cem Concr Res 2010;40:313–20. https://doi.org/10.1016/j.cemconres.2009.09.013.
[59] Ku Y, Ma C-M, Shen Y-S. Decomposition of gaseous trichloroethylene in a photoreactor with TiO_2-coated nonwoven fiber textile. Appl Catal B Environ 2001;34:181–90. https://doi.org/10.1016/S0926-3373(01)00216-8.
[60] Wang H, Wu Z, Zhao W, Guan B. Photocatalytic oxidation of nitrogen oxides using TiO_2 loading on woven glass fabric. Chemosphere 2007;66:185–90. https://doi.org/10.1016/j.chemosphere.2006.04.071.
[61] Zhao J, Yang X. Photocatalytic oxidation for indoor air purification: a literature review. Build Environ 2003;38:645–54. https://doi.org/10.1016/S0360-1323(02)00212-3.
[62] Engel A, Glyk A, Hülsewig A, Große J, Dillert R, Bahnemann DW. Determination of the photocatalytic deposition velocity. Chem Eng J 2015;261:88–94. https://doi.org/10.1016/j.cej.2014.03.040.
[63] Villena G, Lichtenberg N, Lutz V, Jessen W, Klein A, Kurtenbach R, et al. TunNOx: Development and testing of a photocatalytic reactor for efficient NOx-Abatement of Road-Tunnel exhaust. Chem Eng J 2024;490:151832. https://doi.org/10.1016/j.cej.2024.151832.
[64] Verein Deutscher Ingenieure. VDI 3782 Part 5: Environmental Meteorology, Atmospheric Dispersion Models, Deposition Parameters.. https://www.vdi.de/richtlinien/details/vdi-3782-blatt-5-environmental-meteorology-atmospheric-dispersion-models-deposition-parameters.
[65] Bianchi CL, Pirola C, Selli E, Biella S. Photocatalytic NOx abatement: the role of the material supporting the TiO2 active layer. J Hazard Mater 2012;211–212:203–7. https://doi.org/10.1016/j.jhazmat.2011.10.095.
[66] Binas V, Papadaki D, Maggos T, Katsanaki A, Kiriakidis G. Study of innovative photocatalytic cement based coatings: the effect of supporting materials. Constr Build Mater 2018;168:923–30. https://doi.org/10.1016/j.conbuildmat.2018.02.106.
[67] Guo M-Z, Chen J, Xia M, Wang T, Poon CS. Pathways of conversion of nitrogen oxides by nano TiO_2 incorporated in cement-based materials. Build Environ 2018;144:412–8. https://doi.org/10.1016/j.buildenv.2018.08.056.
[68] Jiménez-Relinque E, Rodriguez-Garcia JR, Castillo A, Castellote M. Characteristics and efficiency of photocatalytic cementitious materials: Type of binder, roughness and microstructure. Cem. Concr. Res. 2015;71:124–31. https://doi.org/10.1016/j.cemconres.2015.02.003.
[69] Ballari MM, Satuf ML, Alfano OM. Photocatalytic reactor modeling: application to advanced oxidation processes for chemical pollution abatement. Top Curr Chem 2019;377:22. https://doi.org/10.1007/s41061-019-0247-2.
[70] Boyjoo Y, Sun H, Liu J, Pareek VK, Wang S. A review on photocatalysis for air treatment: from catalyst development to reactor design. Chem Eng J 2017;310:537–59. https://doi.org/10.1016/j.cej.2016.06.090.
[71] Mills A, Andrews R, Han R, O'Rourke C, Hodgen S. Supersensitive test of photocatalytic activity based on ISO 22197–1:2016 for the removal of NO. J Photochem Photobiol A Chem 2020;400:112734. https://doi.org/10.1016/j.jphotochem.2020.112734.
[72] Ballari MM, Yu QL, Brouwers HJH. Experimental study of the NO and NO_2 degradation by photocatalytically active concrete. Catal Today 2011;161:175–80. https://doi.org/10.1016/j.cattod.2010.09.028.
[73] de Lira JOB, Padoin N, Vilar VJP, Soares C. Photocatalytic NOx abatement: Mathematical modeling, CFD validation and reactor analysis. J Hazard Mater 2019;372:145–53. https://doi.org/10.1016/j.jhazmat.2018.07.009.
[74] Lira JOB, Riella HG, Padoin N, Soares C. CFD + DoE optimization of a flat plate photocatalytic reactor applied to NOx abatement. Chem Eng Process - Process Intensif 2020;154:107998. https://doi.org/10.1016/j.cep.2020.107998.
[75] Lira JOB, Riella HG, Padoin N, Soares C. An overview of photoreactors and computational modeling for the intensification of photocatalytic processes in the gas-phase: state-of-art. J Environ Chem Eng 2021;9:105068. https://doi.org/10.1016/j.jece.2021.105068.
[76] Timmerhuis NAB, Wood JA, Lammertink RGH. Connecting experimental degradation kinetics to theoretical models for photocatalytic reactors: the influence of mass transport limitations. Chem Eng Sci 2021;245:116835. https://doi.org/10.1016/j.ces.2021.116835.
[77] ICRI, 2013. 310.2R-2013 BUNDLE (English Book Plus CSP Chip set). ICRI Bookst. https://store.icri.org/item/3102r2013-bundle-english-book-csp-chip-set-342524#tabDates.
[78] Muñoz V, Casado C, Suárez S, Sánchez B, Marugán J. Photocatalytic NOx removal: rigorous kinetic modelling and ISO standard reactor simulation. Catal Today 2019;326:82–93. https://doi.org/10.1016/j.cattod.2018.09.001.
[79] Guo M-Z, Ling T-C, Poon CS. Photocatalytic NOx degradation of concrete surface layers intermixed and spray-coated with nano-TiO_2: influence of experimental factors. Cem Concr Compos 2017;83:279–89. https://doi.org/10.1016/j.cemconcomp.2017.07.022.
[80] Lim TH, Jeong SM, Kim SD, Gyenis J. Photocatalytic decomposition of NO by TiO_2 particles. J Photochem Photobiol A Chem 2000;134:209–17. https://doi.org/10.1016/S1010-6030(00)00265-3.
[81] Nosek Š, Ducháček T, Magyar P, Procházka J. The role of flow structures in the effective removal of NOx pollutants by a TiO_2-based coating in a street canyon. J Environ Chem Eng 2023;11:109758. https://doi.org/10.1016/j.jece.2023.109758.
[82] Jacoby WA, Blake DM, Noble RD, Koval CA. Kinetics of the oxidation of trichloroethylene in air via heterogeneous photocatalysis. J Catal 1995;157:87–96. https://doi.org/10.1006/jcat.1995.1270.
[83] Casagrande CA, Repette WL, Hotza D. Effect of environmental conditions on degradation of NOx gases by photocatalytic nanotitania-based cement mortars after long-term hydration. J Clean Prod 2020;274:123067. https://doi.org/10.1016/j.jclepro.2020.123067.
[84] Toro C, Jobson BT, Haselbach L, Shen S, Chung SH. Photoactive roadways: determination of CO, NO and VOC uptake coefficients and photolabile side product yields on TiO_2 treated asphalt and concrete. Atmos Environ 2016;139:37–45. https://doi.org/10.1016/j.atmosenv.2016.05.007.
[85] Hassan M, Mohammad L, Asadi S, Dylla H, Cooper S. Sustainable photocatalytic asphalt pavements for mitigation of nitrogen oxide and sulfur dioxide vehicle

emissions. J Mater Civ Eng 2013;25:365–71. https://doi.org/10.1061/(ASCE)MT.1943-5533.0000613.

[86] Hernández Rodríguez MJ, Pulido Melián E, González Díaz O, Araña J, Macías M, González Orive A, et al. Comparison of supported TiO_2 catalysts in the photocatalytic degradation of NOx. J Mol Catal A Chem 2016;413:56–66. https://doi.org/10.1016/j.molcata.2015.12.007.

[87] Pill D, Wiesen P, Kleffmann J. Temperature dependencies of the degradation of NO, NO_2 and HONO on a photocatalytic dispersion paint. PCCP 2021;23:9418–27. https://doi.org/10.1039/D1CP01157J.

[88] Huang MH, Huang Y, Cao JJ, Tao WQ. Study on mitigation of automobile exhaust pollution in an urban street canyon: emission reduction and air cleaning street lamps. Build Environ 2021;193:107651. https://doi.org/10.1016/j.buildenv.2021.107651.